Journal of Lasers in Medical Sciences

J Lasers Med Sci 2023;14:e26

Original Article

http://journals.sbmu.ac.ir/jlms

doi 10.34172/jlms.2023.26

Treatment Modelling of a 3D Tumour in Brain by Laser-Induced Interstitial Thermotherapy

Sadegh Amini[1], **Hossein Ahmadikia**[1*]

[1]Mechanical Engineering Department, University of Isfahan, Isfahan, Iran

***Correspondence to**
Hossein Ahmadikia,
Email: ahmadikia@eng.ui.ac.ir

Received: November 29, 2022
Accepted: March 13, 2023
Published online August 22, 2023

Abstract

Introduction: There are some ways to examine heat transfer in tumor tissue, which is an important issue in bioengineering. One of these ways uses the bioheat equation, proposed by Pennes, in a continuous medium. Another one uses a porous medium to model heat transfer in living tissues. The objective of this paper was to study an approach to modelling the temperature distribution and tumour ablation in brain tissue and compare results to Pennes' approach.

Methods: This approach presents and uses a porous medium as the tissue instead of a continuous medium. In addition, the two approaches (simulation in continuous and porous medium) are compared in terms of temperature simulation and amount of cell ablation. The density, heat conduction factor, and blood perfusion rate are considered functions of temperature.

Results: In these approaches, after an 85-second treatment, the temperature increases to about 90°C. The temperature increase of the porous medium is relatively the same as that of the continuous medium and for this reason, the amount of cancerous cells that are ablated in a porous medium is approximately the same as that in a continuous medium. The volume of cell ablation is about 6500 mm^3 for two ideas. In addition, the degree of damage, computed from the Arrhenius integral method, and the ablated volume of the tumour endorse equality at the end of treatment. According to the results, similar to the continuous approach, the porous approach predicts the temperature and amount of volume of damaged cells.

Conclusion: Therefore, it is possible to use the porous approach instead of the Pennes approach for tumour treatment.

Keywords: Ablation; Porous medium; Brain tumour; Laser.

Introduction

Research on heat transfer in living tissue is an important issue that has been studied recently. In 1948, Pennes[1] presented a relatively acceptable equation, named Pennes bioheat equation.[2] After that, many researchers used his equation to simulate heat transfer in living tissues.[3] Pennes introduced an equation by adding a simple scalar source term to the heat transfer equation in solids. This term, named Pennes term, includes the tissue and blood temperatures, blood density and blood perfusion rate in the tissue. Pennes assumed this heat transfer mechanism from blood to tissue. This simplification is one of the main reasons why other researchers used Pennes' theory for modelling heat transfer in living tissues for decades.[4-6] He assumed heat transfer occurs only between arteriole and tissue and ignored the effects of the vein-artery network and blood velocity change in the artery. However, some researchers proposed other heat source terms. Wulff and Klinger[7,8] added a vector source term to the heat transfer equation, assuming that heat transferred from artery to tissue along the artery instead of arteriole to tissue. Some researchers studied the heat transfer mechanism between tissues and arteries and also between arterioles and veins.[9-11] In their studies, the medium is assumed continuous. Besides, there is another idea to model living tissue as a porous medium. Some researchers used the porous medium to model clinical or medical phenomena such as medical imaging, tissue replacement production, and drug delivery.[12] They modeled brain tissue as a porous medium throughout their studies. Some others used the porous medium idea to model brain tissue as a complex aggregate, including two viscous pore liquids, the interstitial fluid and the blood,[13] to simulate multi-component brain tissue numerically in 2D and 3D models.[14,15] Chen presents a brief review of tumor treatment.[16] Riviere-Cazaux et al and Melnick et al studied the effect of laser treatment on primary brain tumors and metastases.[17,18] Rogers et al studied brain tumor treatment by tracing cancerous tissue ablation by magnetic resonance imaging (MRI) technology.[19] Moreover, a laser has been used as an energy source to remove hair from the skin. Some researchers studied this field of science.[20,21] They examined the thermal damage of a laser in different skin types, hair colours, and hair densities. Also, they

Please cite this article as follows: Amini S, Ahmadikia H. Treatment modelling of a 3D tumour in brain by laser-induced interstitial thermotherapy. *J Lasers Med Sci.* 2023;14:e26. doi:10.34172/jlms.2023.26.

optimized spot sizes and pulse durations by simulating the distribution and thermal damage patterns of the laser.

In this article, the effects of the vein-artery network and blood velocity change in arteries on heat transfer in the tumour and brain were evaluated by solving the momentum equation in the tissues. This study was an attempt to model brain tumor ablation by using a porous medium idea to determine the results of this simulation in comparison with Pennes' approach. The arterioles are assumed to be a porous zone, and the remaining parts are assumed to be a matrix zone in the porous medium approach. The walls of arterioles are the boundaries between porous and matrix zones, and heat and mass transfer are modeled by equations diffused through this wall. One of the techniques, used to treat brain tumours in medical sciences, is heating tumor tissue with a source of a laser. Laser-induced interstitial thermotherapy is one of the most famous techniques in this regard.[22] This treatment involves the ablation of cancerous tissues through optic fibres, in which a laser is conducted. The volume of destroyed tissue depends on the absorbed energy and physical and optical properties of the tumour. The photon transportation equation is solved numerically in order to obtain absorbed energy. Then, the transient Pennes equation in the continuous medium and momentum and the heat transfer equations in the porous medium are solved in order to obtain the temperature distribution of the domains. Usually, cells that have experienced temperatures up to 60°C are dead, and the volume of coagulated tissues will be calculated by the Arrhenius integral method.

Methods

Equations

Some studies use and present the Monte Carlo method to simulate laser-skin tissue interaction,[23] but in this study, first, the transport equation of the photon is solved.[24] Then, the distribution of laser intensity is computed in two domains. This equation, which is an integro-differential equation, is solved by a discrete ordinate method to gain photon distribution (intensity distribution of laser $\boldsymbol{I}$, in position $\boldsymbol{r}$ and direction $\boldsymbol{\Omega}$) in the tissue.

The diffusion approximation method is used to evaluate the interaction between light and tissue.

$$(1/C)\left(\partial I(r.t.\Omega.f)/\partial t\right)+\Omega.\nabla I(r.t.\Omega.f) = -\mu_t(r.f)I(r.t.\Omega.f)+\mu_s(r.f)\int \mathrm{P}(\Omega.\Omega')I(r.t.\Omega.f)d\Omega'-I(r.t.\Omega.f) \quad (1)$$

Where, C, t, μ_t, μ_s, and f are light speed in the tissue, time, attenuation coefficient, scattering coefficient, and frequency, respectively.[16] The change of intensity in the tissue is modelled by two left terms. The amount of light, absorbed or scattered by the tissue, is presented by the first term on the right-hand side of the equation. The second term on the right-hand side states the amount of light, which is scattered from another direction (such as $\boldsymbol{\Omega'}$) into the $\boldsymbol{\Omega}$ direction. The last term is a source term such as fluorescence. The amount of energy, absorbed by the tissue, is a function of absorption coefficient μ_a and the summation of light intensity, received by the tissue from all directions. Equation (2) is used to compute the absorbed density of energy per unit volume of tissue:

$$Q_l(r)=\mu_a\int I(r.t.\Omega.f)d\Omega \quad (2)$$

By integrating, the energy density is obtained in the whole tissue. The Brinkman equation (Eq. 3) is solved in a porous medium in order to compute the velocity field. Then, heat transfer equations (4) and (5) in both continuous and porous media are solved, respectively.

Finally, the temperature distribution in the tissue will be obtained.

$$\rho\frac{\partial u}{\partial t}=\nabla.\left[-pI+\frac{\mu}{\varepsilon}\left(\nabla u+(\nabla u)^T\right)\right]-\mu K^{-1}u+\rho g \quad (3)$$

where $\boldsymbol{u}$, p, ρ, μ, ε, and κ are the fluid velocity vector, pressure, fluid density, fluid viscosity, porosity, and permeability tensor of the porous medium, respectively.

$$\rho C_p\frac{\partial T}{\partial t}=\nabla.(k\nabla T)+Q_m+\rho_b C_{p,b}\omega_b(T_b-T)+Q_l \quad (4)$$

$$(\rho C_p)_{eff}\frac{\partial T}{\partial t}=\varepsilon\rho_f C_{p,f}u.\nabla T=\nabla\left(k_{eff}\nabla T\right)=Q_m+Q_l \quad (5)$$

where Q_l is the density of energy produced by the laser in tissue. Q_m is the metabolic source of energy, which is considered zero in comparison with other source terms. ω is the blood perfusion rate in the brain, and the b index refers to blood. k_{eff} and $(\rho C_p)_{eff}$ defined as effective properties in a porous medium are as follows:

$$(\rho C_p)_{eff}=\varepsilon\rho_f C_{p,f}+(1-\varepsilon)\rho_s C_{p,s} \quad and \quad k_{eff}=\varepsilon k_f+(1-\varepsilon)k_s \quad (6)$$

Where ε is porosity, and *eff*, *f*, and *s* indexes refer to the effective, fluid, and solid matrix of a porous medium, respectively.

Another parameter that could show the amount of cell ablation is the degree of damage, according to the Arrhenius integral method (Eq. 7).[25] This parameter is defined as a function of cell concentration in initial time to ablated cell concentration after time τ in a definite tissue.

$$\Omega(\tau)=\ln\left(\frac{C(O)}{C(\tau)}\right)=\int_o^\tau Ae\left(\frac{-E_a}{RT(t)}\right)dt \quad (7)$$

A and E_a are the frequency factor and activation energy for any tissue, R is the universal gas constant, $T(t)$ is the temperature of the tissue, $C(0)$ and $C(\tau)$ are the concentration of undamaged cells in the first and final time of treatment, τ.

Model

Geometry includes a 3D ellipsoid tumour, 20 mm diameters, and 40 mm height, and it is located in an axisymmetric cylinder with a 20 mm radius and 60 mm height as brain tissue (Figure 1). The properties of tumours, brain tissues, and blood are presented in Table 1. There is not any light transportation on the boundaries, except the border of the applicator, which is shown in equation (8). Since the penetration depth of the laser is small and limited to a narrow region near the applicator, it is a reasonable assumption (Table 1)(Figure 1).
The boundary conditions are as bellow in equation (1):

$$I=\begin{cases}\dfrac{50}{0.009\sqrt{2\pi}} & e\left(-(z)^2/\left(2\times.009^2\right)\right) \quad -0.015<z<0.015\\ 0 & \textit{all other boundaies}\end{cases} \tag{8}$$

For transient heat transfer equations (Eqs. 4 and 5) in both continuous and porous approaches, the temperature was fixed at 37°C for all boundaries, except on the tumour-applicator contact border, which is set as heat flux from the model, equal to -15000 W/m^2. Initial conditions are also assumed to be 37°C in the two approaches.

The density and heat conductivity factor of the brain and tumour depends on temperature as follows[32] :

$$k(T)=k_{37}\times\left(1+.00025(T-37)\right) \tag{9}$$

$$\rho(T)=\rho_{37}\times\left(1+.00025(T-37)\right) \tag{10}$$

Where k_{37} and ρ_{37} are the properties of the brain and tumour at 37°C. The Blood perfusion rate is a variable of degree of damage and it is considered in this study.[32]

Table 1. Properties of Brain and Tumour Tissues and Blood[26-31]

Property	Tissue	Value	Unit	Ref.
ρ	Brain	1050	kg/m^3	23
k	Brain	0.528	W/m.K	23
C_p	Brain	3.68	kJ/kg.K	24
μ_a	Brain	40	1/m	24
μ_s	Brain	11000	1/m	24
ω	Brain	0.00477	l/s	25
ρ	Tumour	1040	kg/m^3	23
k	Tumour	0.503	W/m.K	26
C_p	Tumour	3.59	kJ/kg.K	24
μ_a	Tumour	50	1/m	24
μ_s	Tumour	6700	1/m	24
ω	Tumour	0.001	1/s	25
ρ	Blood	1050	kg/m^3	26
C_p	Blood	3.64	kJ/kg.K	26
ε	Brain	0.02	-	27
ε	Tumour	0.02	-	27
A	Tumour & Brain	3.1e98	1/s	28
E_a	Tumour & Brain	6.28e5	J/mol	28

$$\omega_{dynamic}=\omega_{nature}+\left(1-\exp(-\Omega)\right)\left(\omega_{denatured}-\omega_{nature}\right) \tag{11}$$

Where ω_{nature} is the blood perfusion rate in normal conditions and Ω is the degree of damage, which is a function of temperature, and $\omega_{denatured}$ is zero.

Solution Method

The photon transport equation (Eq. 1) is solved in order to evaluate the laser distribution of the whole tumour tissue. The intensity of energy is computed by integrating equation (2) around the spatial angle, used as a source term Q_l in equations 4 and 5. The velocity field of fluid in the porous medium computed by equation (3) is used in equation (5). Therefore, the temperature distribution in the whole domain is obtained by solving equations (4) and (5).

Results

The distribution of laser intensity in the domain is obtained by solving equation (1), as shown in Figure 2. The intensity of the laser, distributed in the tissue or penetrated to the tissue, depends on the active length of the applicator. The amount of penetration of light in the tissues depends inversely on the absorption and scattering coefficients of tissues. Whereas these coefficients are large for a brain, the depth of laser penetration is limited to a very narrow region near the boundaries. As presented in the figure, the affected zone of the laser is limited to nearer regions to the applicator, and then heat transfer mechanisms

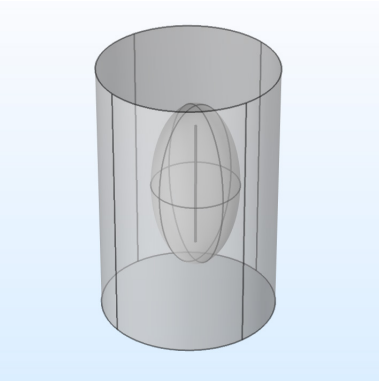

Figure 1. Model of a Brain Tissue and a Tumour

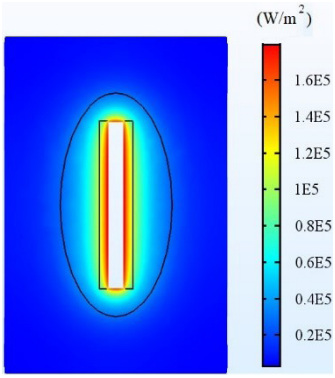

Figure 2. Incident Intensity of the Laser (W/m^2)

transfer energy to other points of the domain.

It is necessary to solve equations (4) and (5) to evaluate the temperature distribution. The heated zone, affected by laser irradiation, is shown in Figure 3. The energy of the laser transfers to the whole domains by some mechanisms, such as conduction and convection. In order to show the temperature details of the two approaches, we presented another diagram. Figure 4a shows the temperature distribution along a line, after 85 seconds. As shown in Figures 3 and 4, the two approaches have the same temperature, approximately.

In addition, it is useful to present temperature at a point in the coordination of $r=4$ and $z=30$ mm by the same power and time. As shown in Figure 4b, when the first and the second techniques are used, the temperature will exceed 90°C. By increasing the temperature, the cells of tissue (healthy and cancerous) will be deformed. Cells that experience temperatures higher than 60°C for about 6 seconds will be coagulated and finally will be dead.[16]

Typically, the area of the tumour, coagulated from laser irradiation, is shown in Figure 5 for the two approaches. The amount of coagulated cells in the two approaches is approximately equal because the temperature distribution of these techniques is the same. Figure 5 shows the distribution of necrosis cells after 85 seconds. As we expected, necrosis cell distribution is the same for the two ideas. In order to compare the number of coagulated cells between the two approaches, the volume of necrosis cells is calculated. The volume of cells, which are coagulated and necrosis in the porous medium through laser irradiation, is presented in Figure 6a, at the end of the treatment process. Another parameter that is used to indicate the volume of ablated tissue is the degree of damage. This parameter indicates the amount of tissue that is ablated to the amount of tissue before ablation at any point. This parameter, as shown in Figure 6b, is computed from the Arrhenius Integral Method. This figure presents the degree of damage to a small diameter

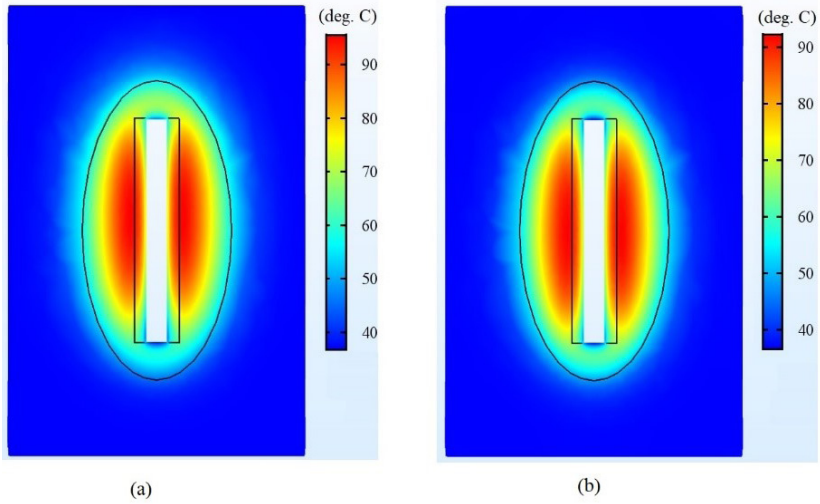

Figure 3. Temperature Distribution After 85 s. (a) Porous approach, (b) Bioheat approach

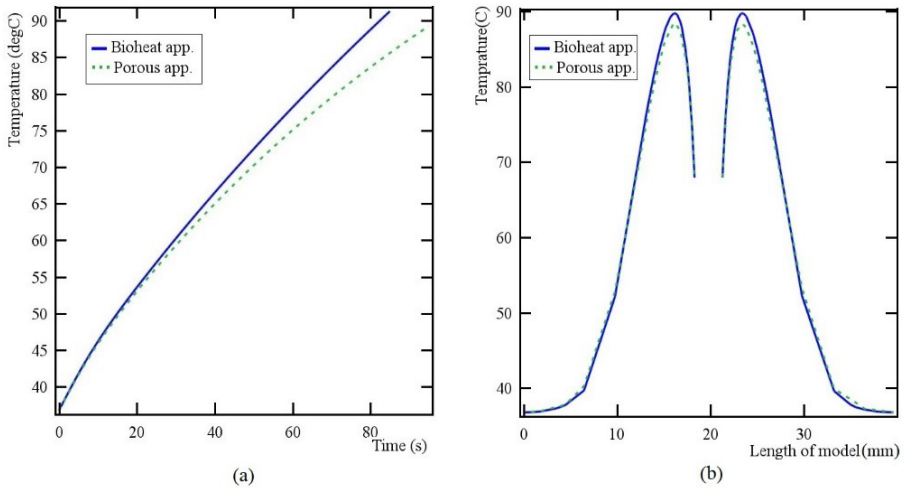

Figure 4. Temperature Distribution (a) at a Line (Small Diameter of Tumour) (b) at a Point (r=4, z=30 mm)

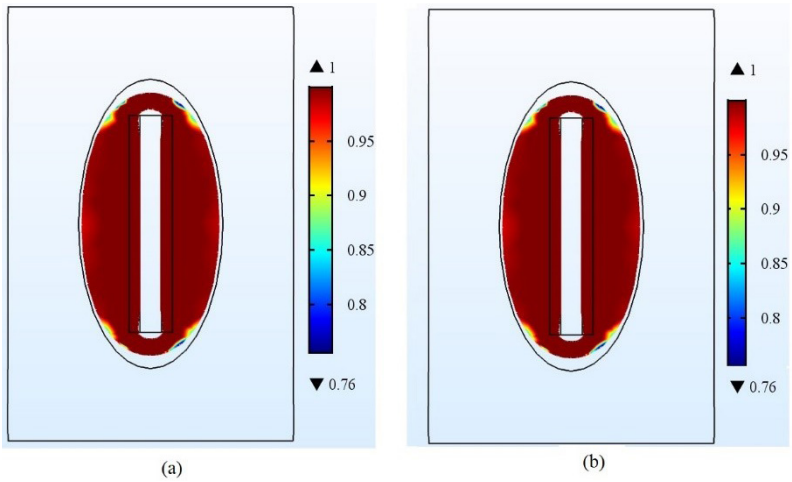

Figure 5. Tumour Ablation (a) porous approach (b) bioheat approach

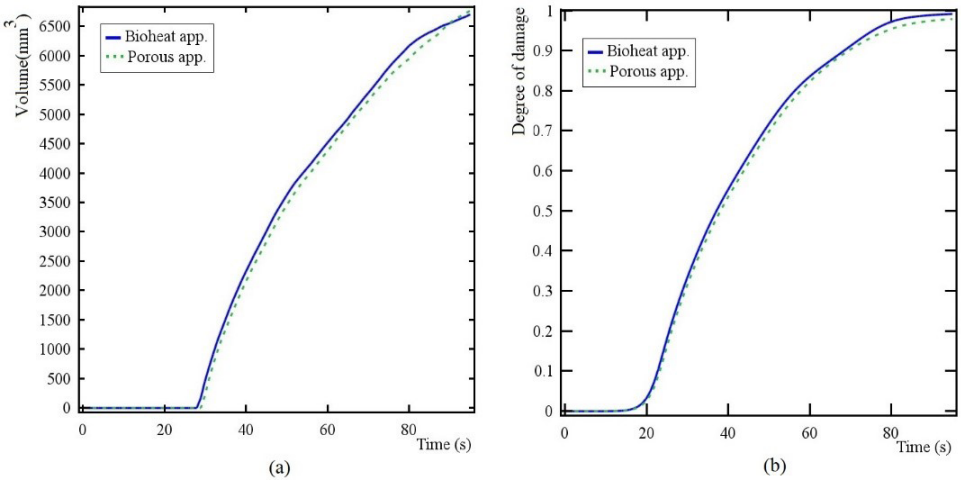

Figure 6. Tumour Ablation (a) volume of ablated cells (b) average degree of damage

of the tumor. According to the diagram, cancerous cells ablated through a porous medium are equal to those ablated through a continuous medium.

Discussion

Nowadays, the ablation of brain tumour is done through heating tissue with energy sources. Pennes simulated the ablation of living tissues in his special approach. The effects of blood perfusion in a continuous medium are added to the heat equation in order to simulate tumour ablation in this approach. Moreover, instead of a continuous medium, a porous medium approach could be an option to the replacement of Pennes' approach. In this study, we attempted to compare two approaches in tumour ablation. First, the photon distribution was computed in the domain by solving the photon transport equation. In order to compare the effect of the medium type, we solved heat transfer equations in the two approaches and then compared temperature distribution at a point and on a line, in Figure 4, respectively. Another matter for comparing the two approaches is the volume of ablated cells by the two methods.

The number of coagulated cells in the continuous and porous mediums is equal. In accordance with the paper, 6700 mm^3 and 6775 mm^3 of tumour cells are coagulated in the porous medium and in the continuous medium, respectively, at the end of the treatment process. The degree of damage is another parameter that is used to indicate the volume of ablated tissue. This parameter indicates the amount of tissue that is ablated in comparison with the amount of tissue before ablation at any point. As shown in Figure 6, this parameter is computed from the Arrhenius integral method. This figure presents an average degree of damage to the tumor. According to the diagram, cancerous cells ablated through a porous medium are equal to those ablated through a continuous medium.

Conclusion

Assuming the brain and its tumor as a porous medium is a way to model brain tumor treatment, instead of continuous medium in Pennes method. In these

approaches, the temperature increases to about 90°C, a safe region, in which the water content of tissue is not vaporized and treatment is done in a good and effective way. In addition, the volume of cell ablation is about 6500 mm^3 for the two ideas. The degree of damage predicts the same in the continuous and porous medium. As shown in the figures, the porous approach predicts the temperature, the amount of volume of damaged cells, and the degree of damage as the continuous approach predicts. Thus, it is possible to use the porous approach instead of the Pennes approach.

Authors' Contribution

Conceptualization: Hossein Ahmadikia, Sadegh Amini.
Formal analysis: Sadegh Amini.
Investigation: Hossein Ahmadikia, Sadegh Amini.
Methodology: Sadegh Amini, Hossein Ahmadikia.
Project administration: Hossein Ahmadikia.
Resources: Hossein Ahmadikia, Sadegh Amini.
Software: Sadegh Amini.
Supervision: Hossein Ahmadikia.
Validation: Hossein Ahmadikia, Sadegh Amini.
Writing–original draft: Sadegh Amini.
Writing–review & editing: Hossein Ahmadikia, Sadegh Amini.

Competing Interests

The authors report no conflict of interest.

References

1. Pennes HH. Analysis of tissue and arterial blood temperatures in the resting human forearm. J Appl Physiol. 1948;1(2):93-122. doi: 10.1152/jappl.1948.1.2.93.
2. Wissler EH. Pennes' 1948 paper revisited. J Appl Physiol (1985). 1998;85(1):35-41. doi: 10.1152/jappl.1998.85.1.35.
3. Bhowmik A, Singh R, Repaka R, Mishra SC. Conventional and newly developed bioheat transport models in vascularized tissues: a review. J Therm Biol. 2013;38(3):107-25. doi: 10.1016/j.jtherbio.2012.12.003.
4. Marqa MF, Colin P, Nevoux P, Mordon SR, Betrouni N. Focal laser ablation of prostate cancer: numerical simulation of temperature and damage distribution. Biomed Eng Online. 2011;10:45. doi: 10.1186/1475-925x-10-45.
5. Fuentes D, Walker C, Elliott A, Shetty A, Hazle JD, Stafford RJ. Magnetic resonance temperature imaging validation of a bioheat transfer model for laser-induced thermal therapy. Int J Hyperthermia. 2011;27(5):453-64. doi: 10.3109/02656736.2011.557028.
6. Olsrud J, Wirestam R, Persson BR, Tranberg KG. Simplified treatment planning for interstitial laser thermotherapy by disregarding light transport: a numerical study. Lasers Surg Med. 1999;25(4):304-14. doi: 10.1002/(sici)1096-9101(1999)25:4<304::aid-lsm5>3.0.co;2-u.
7. Wulff W. Discussion paper: alternatives to the bio-heat transfer equation. Ann N Y Acad Sci. 1980;335:151-4. doi: 10.1111/j.1749-6632.1980.tb50743.x.
8. Klinger HG. Heat transfer in perfused biological tissue. I. General theory. Bull Math Biol. 1974;36(4):403-15. doi: 10.1007/bf02464617.
9. Keller KH, Seiler L Jr. An analysis of peripheral heat transfer in man. J Appl Physiol. 1971;30(5):779-86. doi: 10.1152/jappl.1971.30.5.779.
10. Weinbaum S, Jiji LM, Lemons DE. Theory and experiment for the effect of vascular microstructure on surface tissue heat transfer--part I: anatomical foundation and model conceptualization. J Biomech Eng. 1984;106(4):321-30. doi: 10.1115/1.3138501.
11. Jiji LM, Weinbaum S, Lemons DE. Theory and experiment for the effect of vascular microstructure on surface tissue heat transfer--part II: model formulation and solution. J Biomech Eng. 1984;106(4):331-41. doi: 10.1115/1.3138502.
12. Vadász P. Emerging Topics in Heat and Mass Transfer in Porous Media. Vol 22. Netherlands: Springer; 2008.
13. Ehlers W, Wagner A. Multi-component modelling of human brain tissue: a contribution to the constitutive and computational description of deformation, flow and diffusion processes with application to the invasive drug-delivery problem. Comput Methods Biomech Biomed Engin. 2015;18(8):861-79. doi: 10.1080/10255842.2013.853754.
14. Fink D, Wagner A, Ehlers W. Application-driven model reduction for the simulation of therapeutic infusion processes in multi-component brain tissue. J Comput Sci. 2018;24:101-15. doi: 10.1016/j.jocs.2017.10.002.
15. Amini S, Ahmadikia H. New approach of controlling the area affected in brain tumour treatment by LITT. Comput Methods Biomech Biomed Engin. 2021;24(11):1221-7. doi: 10.1080/10255842.2020.1870966.
16. Chen C, Lee I, Tatsui C, Elder T, Sloan AE. Laser interstitial thermotherapy (LITT) for the treatment of tumors of the brain and spine: a brief review. J Neurooncol. 2021;151(3):429-42. doi: 10.1007/s11060-020-03652-z.
17. Riviere-Cazaux C, Bhandarkar AR, Rahman M, Zheng CR, Bauman MMJ, Naylor RM, et al. Outcomes and principles of patient selection for laser interstitial thermal therapy for metastatic brain tumor management: a multisite institutional case series. World Neurosurg. 2022;165:e520-e31. doi: 10.1016/j.wneu.2022.06.095.
18. Melnick K, Shin D, Dastmalchi F, Kabeer Z, Rahman M, Tran D, et al. Role of laser interstitial thermal therapy in the management of primary and metastatic brain tumors. Curr Treat Options Oncol. 2021;22(12):108. doi: 10.1007/s11864-021-00912-6.
19. Rogers CM, Jones PS, Weinberg JS. Intraoperative MRI for brain tumors. J Neurooncol. 2021;151(3):479-90. doi: 10.1007/s11060-020-03667-6.
20. Ataie-Fashtami L, Shirkavand A, Sarkar S, Alinaghizadeh M, Hejazi M, Fateh M, et al. Simulation of heat distribution and thermal damage patterns of diode hair-removal lasers: an applicable method for optimizing treatment parameters. Photomed Laser Surg. 2011;29(7):509-15. doi: 10.1089/pho.2010.2895.
21. Shirkavand A, Ataie-Fashtami L, Sarkar S, Alinaghizadeh MR, Fateh M, Zand N, et al. Thermal damage patterns of diode hair-removal lasers according to various skin types and hair densities and colors: a simulation study. Photomed Laser Surg. 2012;30(7):374-80. doi: 10.1089/pho.2011.3152.
22. Swami G. Numerical Modeling of Heat Distribution During Laser Tissue Interaction [dissertation]. Rourkela: National Institute of Technology; 2012.
23. Shirkavand A, Sarkar S, Hejazi M, Ataie-Fashtami L, Alinaghizadeh MR. A new Monte Carlo code for absorption simulation of laser-skin tissue interaction. Chin Opt Lett. 2007;5(4):238-40.
24. Niemz MH. Laser-Tissue Interactions: Fundamentals and Applications. 3rd ed. Springer; 2007.
25. Arrhenius S. Über die Reaktionsgeschwindigkeit bei der Inversion von Rohrzucker durch Säuren. Z Phys Chem (N F). 1889;4(1):226-48. doi: 10.1515/zpch-1889-0416.
26. Cooper TE, Trezek GJ. Correlation of thermal properties of some human tissue with water content. Aerosp Med. 1971;42(1):24-7.

27. Taddeucci A, Martelli F, Barilli M, Ferrari M, Zaccanti G. Optical properties of brain tissue. J Biomed Opt. 1996;1(1):117-23. doi: 10.1117/12.227816.
28. Roggan A, Ritz JP, Knappe V, Germer CT, Isbert C, Schädel D, et al. Radiation planning for thermal laser treatment. Med Laser Appl. 2001;16(2):65-72. doi: 10.1078/1615-1615-00012.
29. Schwarzmaier HJ, Yaroslavsky AN, Yaroslavsky IV, Goldbach T, Kahn T, Ulrich F, et al. Optical properties of native and coagulated human brain structures. In: Preceding SPIE 2970, Lasers in Surgery: Advanced Characterization, Therapeutics, and Systems VII. San Jose, CA: SPIE; 1997. p. 492-9. doi: 10.1117/12.275082.
30. Akdogan I, Kiroglu Y, Onur S, Karabuluti N. The volume fraction of brain ventricles to total brain volume: a computed tomography stereological study. Folia Morphol (Warsz). 2010;69(4):193-200.
31. Schwarzmaier HJ, Yaroslavsky IV, Yaroslavsky AN, Fiedler V, Ulrich F, Kahn T. Treatment planning for MRI-guided laser-induced interstitial thermotherapy of brain tumors--the role of blood perfusion. J Magn Reson Imaging. 1998;8(1):121-7. doi: 10.1002/jmri.1880080124.
32. Nour M, Oukaira A, Bougataya M, Lakhssassi A. Thermal damage modeling analysis and validation during treatment of tissue tumors. Int J Pharma Med Biol Sci. 2017;6(4):98-104. doi: 10.18178/ijpmbs.6.4.98-104.